

Systemic Microvascular Dysfunction and Inflammation after Pulmonary Particulate Matter Exposure

Timothy R. Nurkiewicz,^{1,2} Dale W. Porter,^{1,3} Mark Barger,³ Lyndell Millecchia,³ K. Murali K. Rao,³ Paul J. Marvar,^{1,2} Ann F. Hubbs,³ Vincent Castranova,^{1,3} and Matthew A. Boegehold^{1,2}

¹Department of Physiology and Pharmacology, and ²Center for Interdisciplinary Research in Cardiovascular Sciences, West Virginia University School of Medicine, Morgantown, West Virginia, USA; ³Pathology and Physiology Research Branch, Health Effects Laboratory Division, National Institute for Occupational Safety and Health, Morgantown, West Virginia, USA

The epidemiologic association between pulmonary exposure to ambient particulate matter (PM) and cardiovascular dysfunction is well known, but the systemic mechanisms that drive this effect remain unclear. We have previously shown that acute pulmonary exposure to PM impairs or abolishes endothelium-dependent arteriolar dilation in the rat spinotrapezius muscle. The purpose of this study was to further characterize the effect of pulmonary PM exposure on systemic microvascular function and to identify local inflammatory events that may contribute to these effects. Rats were intratracheally instilled with residual oil fly ash (ROFA) or titanium dioxide at 0.1 or 0.25 mg/rat 24 hr before measurement of pulmonary and systemic microvascular responses. *In vivo* microscopy of the spinotrapezius muscle was used to study systemic arteriolar responses to intraluminal infusion of the Ca²⁺ ionophore A23187 or iontophoretic abluminal application of the adrenergic agonist phenylephrine (PHE). Leukocyte rolling and adhesion were quantified in venules paired with the studied arterioles. Histologic techniques were used to assess pulmonary inflammation, characterize the adherence of leukocytes to systemic venules, verify the presence of myeloperoxidase (MPO) in the systemic microvascular wall, and quantify systemic microvascular oxidative stress. In the lungs of rats exposed to ROFA or TiO₂, changes in some bronchoalveolar lavage markers of inflammation were noted, but an indication of cellular damage was not found. In rats exposed to 0.1 mg ROFA, focal alveolitis was evident, particularly at sites of particle deposition. Exposure to either ROFA or TiO₂ caused a dose-dependent impairment of endothelium-dependent arteriolar dilation. However, exposure to these particles did not affect microvascular constriction in response to PHE. ROFA and TiO₂ exposure significantly increased leukocyte rolling and adhesion in paired venules, and these cells were positively identified as polymorphonuclear leukocytes (PMNLs). In ROFA- and TiO₂-exposed rats, MPO was found in PMNLs adhering to the systemic microvascular wall. Evidence suggests that some of this MPO had been deposited in the microvascular wall. There was also evidence for oxidative stress in the microvascular wall. These results indicate that after PM exposure, the impairment of endothelium-dependent dilation in the systemic microcirculation coincides with PMNL adhesion, MPO deposition, and local oxidative stress. Collectively, these microvascular observations are consistent with events that contribute to the disruption of the control of peripheral resistance and/or cardiac dysfunction associated with PM exposure. **Key words:** arteriole, endothelium, microcirculation, myeloperoxidase, oxidative stress, particulate matter, polymorphonuclear leukocyte, systemic, venule. *Environ Health Perspect* 114:412–419 (2006). doi:10.1289/ehp.8413 available via <http://dx.doi.org/> [Online 13 October 2005]

Epidemiologic studies have suggested that exposure to particulate air pollution may result in as many as 100,000 premature deaths per year in the United States (Schwartz et al. 2002). Multiple studies over a broad range of geographical locations indicate that for each 10 µg/m³ increase in ambient particulate matter (PM), the daily mortality rate is augmented by approximately 1–5% (Pope et al. 2002; Schwartz et al. 1996). Mortality due to cardiovascular complications after acute PM exposure comprises a significant component of all-cause mortality (Goldberg et al. 2001; Samet et al. 2000). The U.S. population continues to grow; at least two-thirds of our population is obese or overweight (Hedley et al. 2004), and now one-third is hypertensive (Fields et al. 2004). Children and senior citizens comprise approximately 40% of the total U.S. population, and this figure is projected to swiftly increase in the

coming years (U.S. Census Bureau 2004.). A major concern is that despite the ongoing growth of the most susceptible populations, the mechanisms by which PM increases morbidity and mortality remain largely unknown.

Three prominent hypotheses have been advanced to explain how pulmonary PM exposure can elicit a cardiovascular response (Brook et al. 2004; Nemmar et al. 2002; Oberdorster et al. 2004). The first hypothesis proposes that PM deposited in the lung acts through a neural mechanism to alter central nervous system function. In the lung, nociceptive neurons are stimulated by residual oil fly ash (ROFA) (Veronesi et al. 2000). Cardiac autonomic function is also altered by PM exposure, suggesting that central input to the heart is altered (Chen and Hwang 2005). Acute electrocardiographic changes after PM exposure are also suggestive of an activated neural mechanism

(Wichers et al. 2004). The second hypothesis proposes that PM deposited in the lung gains access to the systemic circulation and directly interacts with target tissues. After exposure, PM deposition has been reported in a variety of extrapulmonary tissues, including the blood, ventricular microvascular walls, liver, spleen, heart, and brain (Calderon-Garciduenas et al. 2001; Kreyling et al. 2002; Nemmar et al. 2001, 2002; Oberdorster et al. 2002, 2004). No study has shown *in vivo* that the presence of particles within a peripheral tissue is detrimental to its function, but several lines of evidence support this hypothesis. In Mexico City canines, PM deposition was found in the cardiac arteriolar wall where polymorphonuclear leukocyte (PMNL) margination and microthrombi were also observed (Calderon-Garciduenas et al. 2001). Although not truly representative of PM exposure and subsequent deposition, treatment of cells or tissues *in vitro* with PM causes cytokine and tumor necrosis factor- α (TNF- α) production, cytotoxicity via endotoxins, oxidative stress, and smooth muscle relaxation (Bagate et al. 2004; Dye et al. 1997; Li et al. 2003; Osornio-Vargas et al. 2003; van Eeden et al. 2001). The third hypothesis proposes that PM deposited in the lung initiates a local inflammatory response that develops into a systemic inflammatory response, characterized by alterations in circulating factors and cells associated with inflammation. Pulmonary inflammation after PM exposure is well documented by our laboratory and many others, in animals as well as humans (Dreher et al. 1997; Nurkiewicz et al. 2004; Schaumann et al. 2004). Circulating

Address correspondence to T.R. Nurkiewicz, Department of Physiology and Pharmacology, Box 9229, Robert C. Byrd Health Sciences Center, West Virginia University, Morgantown, WV 26506-9229 USA. Telephone: (304) 293-7328. Fax: (304) 293-5513. E-mail: tnurkiewicz@hsc.wvu.edu

We thank K. Wix for her expert technical assistance in this study.

The findings and conclusions in this report are those of the authors and do not necessarily represent the views of the National Institute for Occupational Safety and Health.

This work was supported by the National Institutes of Health (Research Service Award HL-67562 to T.R.N. and RO1 HL-44012 to M.A.B.).

The authors declare they have no competing financial interests.

Received 20 June 2005; accepted 12 October 2005.

interleukin (IL)-1 and IL-6 are elevated in humans exposed to PM (van Eeden et al. 2001). IL-1, TNF- α , and the immune-related transcription factor nuclear factor κ B are elevated in the brain tissue of mice exposed to PM (Campbell et al. 2005). Furthermore, blood samples from healthy humans exposed to PM reveal elevations in immature PMNL, neutrophils, and platelets (Salvi et al. 1999; Tan et al. 2000).

Although the evidence for these three hypotheses is substantial, and end points have been identified in some cases, the ultimate basic mechanisms responsible for perturbations in a given system are unclear. We have previously shown that PM exposure impairs or abolishes systemic endothelium-dependent arteriolar dilation and dramatically increases venular leukocyte adhesion and rolling (Nurkiewicz et al. 2004). As part of a logical and methodic progression toward identifying these basic mechanisms, we undertook the present study to expand our previous findings in the systemic microvasculature and better characterize the remote effects of pulmonary PM exposure on the spinotrapezius muscle microcirculation. We hypothesized that after PM exposure, events linked to inflammation, such as hemoprotein deposition and oxidative stress, should be present at the microvascular level.

Experimental objectives. Our first objective was to determine if alteration of systemic microvascular function can occur after pulmonary PM exposure at levels that fail to cause gross pulmonary toxicity. Rats were exposed by intratracheal (IT) instillation to various doses of ROFA, titanium dioxide, or saline. We assessed pulmonary inflammation and damage by measuring bronchoalveolar lavage (BAL) parameters and evaluated systemic microvascular function by intravital microscopy of spinotrapezius muscle arterioles. Microvascular reactivity was determined by measurement of dilator responsiveness to endothelial stimulation.

Our second objective was to determine if the effects of pulmonary PM exposure on systemic microvascular reactivity to vasodilators are due to an enhanced vasopressor effect via modification of adrenergic responsiveness. Rats were treated with saline or 0.25 mg ROFA by IT instillation. Spinotrapezius muscle arterioles were studied by intravital microscopy. Adrenergic responsiveness was determined by measurement of constrictor responsiveness after α_1 -adrenergic receptor stimulation.

Our third objective was to identify events in the lung, blood, and systemic microcirculation that are consistent with inflammation after PM exposure. Rats were treated with saline or various doses of ROFA or TiO₂ by IT instillation. We evaluated the number of rolling and adherent leukocytes in spinotrapezius muscle venules, lung histology, muscle histology, microvascular mRNA levels, myeloperoxidase

(MPO) deposition, and oxidative stress in the spinotrapezius muscle microvascular wall.

Materials and Methods

PM preparation. ROFA was collected from a precipitator at Boston Edison Co., Mystic Power Plant number 4 (Everett, MA). ROFA particle size and elemental composition from this source have been previously characterized (Antonini et al. 2002; Roberts et al. 2004). ROFA particles were of respirable size with a count mean diameter of 2.2 μ m. We used TiO₂ (mean diameter of 1 μ m; Aldrich, Milwaukee, WI) to determine if any ROFA effects were substance specific. ROFA and TiO₂ samples (suspended in 300 μ L sterile saline) were sonicated for 1 min before IT instillation.

Experimental animals. Male Sprague Dawley rats (7–8 weeks of age) were purchased from Harlan Sprague Dawley (Indianapolis, IN) and housed at the West Virginia University Health Sciences Center in an animal facility approved by the Association for Assessment and Accreditation of Laboratory Animal Care. To ensure that all methods were performed humanely and with regard for alleviation of suffering, all experimental procedures were approved by the West Virginia University Animal Care and Use Committee.

IT instillation. Rats were lightly anesthetized by an intraperitoneal (ip) injection of sodium methohexital and IT instilled with ROFA (0.1 or 0.25 mg/rat) according to previously established methods (Brain et al. 1976). We have previously shown that these doses partially impair or completely abolish endothelium-dependent arteriolar dilation in the rat spinotrapezius muscle (Nurkiewicz et al. 2004). Rats in the vehicle control group were IT dosed with 300 μ L sterile saline. Rats in the particle control group were dosed with TiO₂ (0.1 or 0.25 mg/rat). After IT instillation, all rats recovered for 24 hr before BAL, histology, or intravital microscopy experiments.

Collection of BAL samples for measurement of pulmonary inflammation and damage. Rats were euthanized with sodium pentobarbital (≥ 100 mg/kg, ip). A tracheal cannula was inserted, and BAL was performed through the cannula using ice-cold Ca²⁺/Mg²⁺-free phosphate-buffered saline as previously described (Nurkiewicz et al. 2004).

BAL fluid lactate dehydrogenase (LDH) activity and albumin protein assays. BAL fluid LDH activities were determined as a marker of cytotoxicity, and albumin concentrations were determined as an indicator of the integrity of the alveolar air–blood barrier. Both assays were measured as previously described (Nurkiewicz et al. 2004).

Alveolar macrophage (AM) chemiluminescence (CL). AM CL was determined as previously described (Nurkiewicz et al. 2004)

to evaluate reactive oxygen species production by AM.

Histology and immunohistochemistry. To more thoroughly identify pulmonary inflammation, microscopic sections of lungs from rats treated with saline or exposed to 0.1 mg ROFA were evaluated. Lung tissue sections were evaluated by a board-certified veterinary pathologist for morphologic alterations. Semi-quantitative pathology scores were calculated for alveolar inflammation in each slide. The pathology score was the sum of numeric conversion of the severity (none, minimal, mild, moderate, marked, or severe) and distribution (none, focal, locally extensive, multifocal, multifocal and coalescent, or severe) of tissue alterations to produce a pathology score on a scale of 0–10 (Porter et al. 2001).

To characterize cell types associated with systemic microvascular inflammation, histologic analysis was performed on the spinotrapezius muscle of rats 24 hr after exposure to ROFA or TiO₂ (0.1 or 0.25 mg for each particle type). The muscle was removed from the rat, fixed immediately in 10% formalin, processed, and embedded in paraffin. Paraffin sections stained with hematoxylin and eosin (H&E) allowed positive identification of neutrophils and eosinophils.

To localize the hemoprotein MPO in the spinotrapezius muscle of rats 24 hr after treatment with saline or 0.25 mg ROFA, immunohistochemistry was performed as previously described (Eiserich et al. 2002). Sections were deparaffinized and, after microwave antigen retrieval in citrate buffer pH 6, were incubated overnight at 4°C with a polyclonal antibody against MPO (1:500; Calbiochem, EMD Biosciences Inc., La Jolla, CA). An Alexa 488 fluorescent-conjugated goat anti-rabbit secondary antibody (Molecular Probes, Eugene, OR) was used to localize MPO. After counterstaining the nuclei with diamidinophenylindole (DAPI; Molecular Probes), sections were examined with a Zeiss LSM 510 laser scanning confocal microscope system (Carl Zeiss Inc., Thornwood, NY).

Reverse transcriptase–polymerase chain reaction (RT-PCR). The left and right spinotrapezius muscles were excised from rats 24 hr after treatment with saline or 0.25 mg ROFA, and the microcirculation was dissected from the surrounding skeletal muscle. The pooled microvascular samples from an individual rat were stored in RNAlater (Ambion, Austin, TX) at 4°C for total RNA isolation. Total RNA was isolated using an Array Pure Nano-scale RNA Purification Kit (Epicentre, Madison, WI) and analyzed as previously described (Rao et al. 2004).

Intravital microscopy. Rats were anesthetized with sodium thiopental (100 mg/kg, ip) and placed on a heating pad to maintain a 37°C rectal temperature. The trachea was

intubated to ensure a patent airway, and the right carotid artery was cannulated to measure arterial pressure. The right spinotrapezius muscle was then exteriorized, superfused with an electrolyte solution, and prepared for microscopic observation as previously described (Nurkiewicz et al. 2004).

The animal preparation was then transferred to the stage of an intravital microscope. Video images were displayed and videotaped for off-line analysis. During videotape replay, arteriolar inner diameters were measured and venular leukocyte adhesion was quantified.

Experimental protocols. Protocol 1. Arteriolar endothelium-dependent dilation was evaluated by assessing the capacity for Ca²⁺-dependent endothelial nitric oxide formation in response to intraluminal infusion of the calcium ionophore A23187 (Sigma Chemical Co., St. Louis, MO). Glass micropipettes were filled with a 10⁻⁷ M solution of A23187 and inserted into the arteriolar lumen, and A23187

was then infused directly into the flow stream for 2-min periods at ejection pressures of 5, 10, 20, and 40 psi (Nurkiewicz et al. 2004). A 2-min recovery period followed each ejection. At the end of all intravital experiments, adenosine (ADO) was added to the superfusate (10⁻⁴ M final concentration) to fully dilate the microvascular network and determine the passive diameter of each arteriole studied.

Protocol 2. To evaluate arteriolar responsiveness to adrenergic stimulation, phenylephrine (PHE) was iontophoretically applied to individual arterioles in rats after exposure to either saline or 0.25 mg ROFA. Micropipettes were filled with a 50-mM solution of PHE in distilled water. The pipette tip was placed in light contact with the arteriolar wall, and a current programmer delivered continuous 2-min ejection currents of 50, 100, and 200 nA (randomly). A 2-min recovery period followed each application. To exclude the possibility that adrenergic stimulation could increase NO

production and therefore attenuate the observed constrictions, these experiments were performed during NO synthase (NOS) inhibition with N^G-monomethyl-L-arginine (10⁻⁴ M final superfusate concentration).

Protocol 3. Adhering or rolling leukocytes in first-order venules of rats after exposure to either saline, 0.25 mg ROFA, or 0.1 mg TiO₂ were quantified to characterize microvascular inflammation. Leukocytes that were either stationary or moving but in constant contact with the venular wall for at least 200 μm were counted for 1 min in each venule studied.

Protocol 4. Oxidant activity in the arteriolar wall was measured with the tetranitroblue tetrazolium (TNBT) reduction method, which provides a general index of microvascular oxidant stress (Lenda and Boegehold 2002). After 1 hr of continuous exposure to 2% TNBT superfusion, the spinotrapezius muscle was fixed with a 10% formalin solution and excised. The tissue was then viewed with bright-field microscopy, and images of microvessels were digitized and analyzed. Using a 1 × 5 μm photometric window, a series of average pixel intensity measurements were made along the vessel wall and in extravascular regions immediately adjacent to the wall. To assess microvascular wall levels of formazan (the reduction product of TNBT and therefore an index of oxidant activity), the measured pixel intensities were used to calculate microvascular wall light absorption (*A*): $A = \ln(I_t/I_o)$, where *I_t* is the vessel intensity and *I_o* is the intensity for the adjacent extravascular region. The amount of formazan formed is proportional to the level of oxidant activity, and calculated light absorption is linearly related to the amount of formazan present (Lenda and Boegehold 2002).

Data and statistical analyses. Arteriolar diameter (*D*, in micrometers) was sampled at 10-sec intervals. Resting vascular tone was calculated for each vessel as follows: $\text{tone} = [(D_{\text{pass}} - D)/D_{\text{pass}}] \times 100$, where *D_{pass}* is

Table 1. Profiles of experimental animals used for intravital studies.

Experimental group	<i>N</i>	Age (days)	Weight (g)	Mean arterial pressure (mm Hg)
Saline control	15	55 ± 4	236 ± 4	98 ± 5
0.1 mg TiO ₂	5	50 ± 1	275 ± 9*	108 ± 6
0.1 mg ROFA	4	52 ± 1	225 ± 3	102 ± 9
0.25 mg TiO ₂	3	56 ± 3	219 ± 7	91 ± 15
0.25 mg ROFA	11	50 ± 2	221 ± 8	94 ± 7

N, number of rats. Values are mean ± SE. **p* < 0.05 compared with all other groups.

Table 2. BAL data from saline-treated and TiO₂- and ROFA-exposed rats.

Experimental group	Cellular content of PMNL (10 ⁶ cells/rat)	BAL fluid		Total AM CL
		Albumin (mg/mL)	LDH (U/L)	
Saline control	0.93 ± 0.11	0.13 ± 0.02	58 ± 10	7.50 ± 1.63
0.1 mg TiO ₂	1.73 ± 0.36*	0.14 ± 0.04	67 ± 13	5.21 ± 1.60
0.1 mg ROFA	1.24 ± 0.28	0.23 ± 0.05	75 ± 2	14.47 ± 2.60*,**
0.25 mg TiO ₂	1.11 ± 0.15	0.19 ± 0.02	65 ± 8	3.64 ± 0.73
0.25 mg ROFA	1.91 ± 0.20*	0.17 ± 0.01	46 ± 4	17.42 ± 1.11*,**

N = 22 rats for saline control; *N* = 5–7 rats for all other doses. Values are mean ± SE. CL = counts per minute × 10⁵/0.25 × 10⁶ AM/15 min.

p* < 0.05 compared with saline. *p* < 0.05 compared with 0.1 mg TiO₂ and *p* < 0.05 compared with 0.25 mg TiO₂.

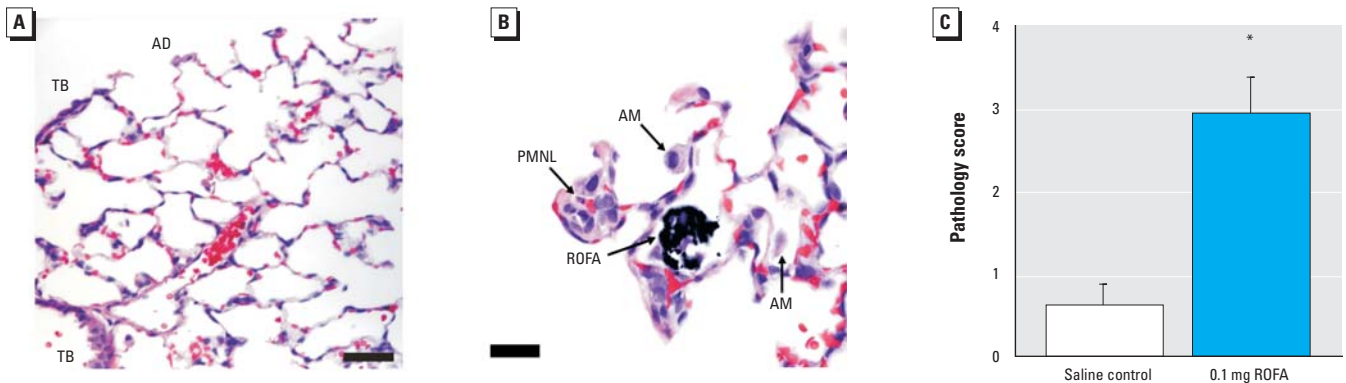


Figure 1. Histologic evidence of focal pulmonary alveolitis 24 hr after PM exposure. (A) and (B) are representative findings from five saline-treated rats and five rats exposed to 0.1 mg ROFA. (A) Saline control showing no morphologic alterations. Abbreviations: AD, alveolar duct; TB, terminal bronchioles. Bar = 50 μm. (B) Histopathologic alterations in a ROFA-exposed rat. Agglomerated ROFA particles in an alveolar space can be seen near an alveolar duct. The ROFA particles do not transmit light and therefore appear black when viewed in the light microscope. AMs are frequently observed in alveoli near ROFA particles and are intimately associated with the agglomerated ROFA. PMNLs are present in lesser numbers near ROFA particles, most frequently in the interstitium. Bar = 20 μm. (C) Mean alveolitis pathology scores.

**p* < 0.05 compared with saline; similar results were obtained with TiO₂.

passive diameter under ADO, and D_c is the diameter measured during the control period. A tone of 100% represents complete vessel closure, whereas 0% represents the passive state. All data are reported as mean \pm SE, where n represents the number of arterioles and N represents the number of rats. Statistical analysis was performed by commercially available software (Sigmastar; Jandel Scientific, Chicago, IL). We used one-way repeated-measures analysis of variance (ANOVA) to determine the effect of a treatment within a group or differences among groups. Two-way repeated-measures ANOVA was used to determine the effects of group, treatment, and group \times treatment interactions on measured variables. For all ANOVA procedures, we used the Student-Newman-Keuls method for post hoc analysis to isolate pairwise differences among specific groups. Significance was assessed at the 95% confidence level ($p < 0.05$) for all tests.

Results

The general characteristics of rats used for intravital microscopy experiments are reported in Table 1. At the time of study, age and mean arterial pressure were not different among the experimental groups. Body weight was significantly higher in the 0.1-mg TiO₂ group. Rats used for BAL data were of the same age as those reported in Table 1 (data not shown).

The effects of pulmonary exposure to ROFA and TiO₂ on BAL parameters of inflammation and damage 24 hr after IT treatment are reported in Table 2. PMNL counts were significantly higher in the 0.1-mg TiO₂ and 0.25-mg ROFA groups than in the saline-treated group, but not in the 0.25-mg TiO₂ and 0.1-mg ROFA groups. BAL fluid albumin and LDH were not significantly different among the experimental groups. Total zymosan-stimulated AM CL was significantly greater in the 0.1-mg ROFA and 0.25-mg ROFA groups than that in the saline controls, whereas the 0.1-mg and 0.25-mg TiO₂ groups were not different from the saline controls. AM counts were not statistically different among the experimental groups (data not shown).

The pulmonary microscopic sections of five saline-treated rats and five rats exposed to 0.1 mg ROFA were examined by a board-certified veterinary pathologist at 24 hr post-exposure. Figure 1A represents a typical slide from saline-treated rats, in which no morphologic alterations are present. Erythrocytes were occasionally present in slides from saline-treated rats, but this was an artifact of the fixation

technique. The alveolitis was predominantly histiocytic, although lesser numbers of neutrophils and/or eosinophils were sometimes observed. Alveolitis was generally centered around alveolar ducts or perivascular spaces near alveolar ducts in all rats. In several foci of alveolitis, agglomerated ROFA could be seen in association with alveolar inflammation (Figure 1B). The mean alveolitis pathology score of 2.92 ± 0.43 in ROFA-exposed rats was significantly greater than that for saline-treated rats (0.60 ± 0.27 ; Figure 1C).

Resting variables of all arterioles studied 24 hr postexposure are reported in Table 3. Resting and passive (in the presence of ADO) arteriolar diameters were not significantly different among the experimental groups. Accordingly, resting arteriolar tone was not different among the experimental groups.

In spinotrapezius muscle arterioles of the saline-treated group, A23187 infusion produced dose-dependent dilation that was near maximal at the highest ejection pressure (Figure 2). Exposure to 0.25 mg TiO₂ or ROFA completely abolished this response 24 hr postexposure at each ejection pressure. Arterioles in rats exposed to 0.1 mg TiO₂ or ROFA displayed an attenuated responsiveness to A23187 infusion. In these groups, vasodilation in response to A23187 infusion at 20 and 40 psi was significantly greater than that observed in rats exposed to either particle at 0.25 mg. Additionally, the response in the 0.1 mg TiO₂ group at 10 psi was significantly greater than that observed for either group at 0.25 mg. These findings support our original observations and are consistent with our postulate that pulmonary exposure to PM inhibits systemic microvascular function in a dose-dependent manner (Nurkiewicz et al. 2004).

Arteriolar adrenergic sensitivity 24 hr after PM exposure was assessed with PHE application and resultant vasoconstriction (Figure 3). Iontophoretic PHE application produced robust, dose-dependent arteriolar constriction in saline-treated rats. In rats exposed to 0.25 mg ROFA (a pulmonary load that abolished endothelium-dependent dilation), the arteriolar responses to PHE iontophoresis were identical to those in saline-treated rats. This suggests that after pulmonary PM exposure, peripheral arterioles are not hypersensitive to adrenergic stimulation and that their contractile ability is unaltered.

The number of rolling and adherent leukocytes through 200 μ m venular segments is displayed in Figure 4. We have previously

reported this number to be as great as 54 ± 4 leukocytes/min in rats exposed to 2 mg ROFA (Nurkiewicz et al. 2004). This systemic response to PM exposure is widespread throughout the microvascular network and is significantly greater than that observed in venules of saline-treated rats (13 ± 2 leukocytes/min). Results in the present study indicate that, at 24 hr postexposure, this dynamic response persists at equivalent magnitudes in venules of rats exposed to either 0.25 mg ROFA or 0.1 mg TiO₂ (52 ± 5 or 65 ± 9 leukocytes/min, respectively).

Spinotrapezius muscle histology was performed to specifically identify the adherent and rolling leukocytes reported in Figure 4. Rats were either treated with saline or exposed to 0.1 mg ROFA. At 24 hr postexposure, the

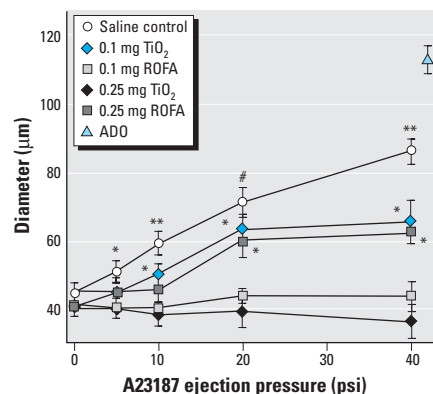


Figure 2. PM exposure impairs or abolishes spinotrapezius muscle arteriolar responsiveness to intraluminal A23187 in a dose-dependent manner 24 hr after IT treatment. n , number of arterioles. Saline control, $n = 13$; 0.1 mg TiO₂, $n = 9$; 0.1 mg ROFA, $n = 9$; 0.25 mg TiO₂, $n = 8$; 0.25 mg ROFA, $n = 8$. Maximum diameter obtained with ADO (10^{-4} M, final superfusate concentration). Values are mean \pm SE. * $p < 0.05$ compared with 0.25 mg TiO₂ and 0.25 mg ROFA. ** $p < 0.05$ compared with 0.1 mg TiO₂, 0.1 mg ROFA, 0.25 mg TiO₂, and 0.25 mg ROFA. # $p < 0.05$ compared with 0.1 mg ROFA, 0.25 mg TiO₂, and 0.25 mg ROFA.

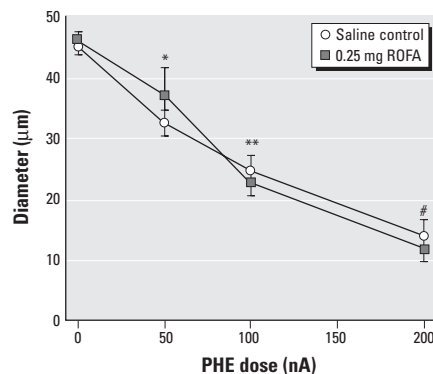


Figure 3. ROFA exposure does not alter arteriolar vasopressor responsiveness to PHE in the spinotrapezius muscle. n , number of arterioles. Saline control, $n = 8$; 0.25 mg ROFA, $n = 8$. Values are mean \pm SE. * $p < 0.05$ compared with 0 nA in both groups; ** $p < 0.05$ compared with 50 nA in both groups; # $p < 0.05$ compared with 100 nA in both groups.

Table 3. Resting variables for all arterioles studied (mean \pm SE).

	Saline	0.1 mg TiO ₂	0.1 mg ROFA	0.25 mg TiO ₂	0.25 mg ROFA
No. of arterioles	28	9	9	8	25
Resting diameter (μ m)	44 \pm 2	45 \pm 1	41 \pm 2	41 \pm 2	43 \pm 1
Passive diameter (μ m)	108 \pm 3	111 \pm 4	111 \pm 6	100 \pm 3	106 \pm 3
Resting tone (% of maximum)	59 \pm 2	59 \pm 2	62 \pm 3	59 \pm 2	59 \pm 1

muscles were excised, fixed, and stained with H&E (Figure 5). Histologic analysis positively identified the adherent cells in venules from ROFA-exposed rats as PMNLs because of the presence of deeply lobed nuclei. Identical results were obtained in rats exposed to TiO₂ (data not shown).

RT-PCR was performed to characterize potential inflammatory markers at the systemic microvascular level after PM exposure (Figure 6). Rats were either treated with saline or exposed to 0.25 mg ROFA 24 hr before spinotrapezius muscle microvessel dissection. Although no inflammatory marker was different between the two groups, it is important to note that neither endothelial NOS (eNOS) nor inducible NOS (iNOS) message was altered by PM exposure. This suggests that the capacity of microvascular endothelium to synthesize eNOS is not impaired after PM exposure.

To further characterize inflammatory events associated with venular PMNL adhesion

24 hr after PM exposure, we identified the presence of MPO in neutrophils and the microvascular wall in the spinotrapezius muscle (Figure 7). Representative confocal fluorescence images are presented in Figure 7. In Figure 7A, MPO is evident (intense green fluorescence) in a single PMNL of a saline-treated rat. In Figure 7B, MPO is evident not only in each of the multiple PMNLs but also in the microvascular wall of a rat exposed to 0.25 mg ROFA. It is also apparent in Figure 7B that some PMNLs have migrated, or are in the process of migrating, from the microvascular lumen into the interstitial space. Similar results were observed in rats exposed to TiO₂ (data not shown). This histologic and immunologic evidence suggests that MPO deposition occurs in the systemic microvascular wall after pulmonary PM exposure.

To better characterize the effects of systemic inflammation associated with PM exposure, general oxidative stress was measured in

the spinotrapezius muscle microvascular wall 24 hr after IT treatment (Figure 8). Calculated light absorption (from deposits of formazan, the reduction product of TNBT and reactive oxygen species) in the microvascular wall from rats exposed to 0.25 mg ROFA was significantly greater than that from saline-treated rats. This suggests that general oxidative stress in the systemic microcirculation increases after pulmonary PM exposure.

Discussion

This second report from our group is part of our ongoing investigation of the remote biologic effects at the systemic microvascular level that follow pulmonary PM exposure. In the present study, we present three novel observations. Additionally, we have verified our previous findings using lower PM doses.

We have previously reported that exposure to ROFA produces a dose-dependent impairment of systemic endothelium-dependent arteriolar dilation and increases venular leukocyte adhesion and rolling (Nurkiewicz et al. 2004). This arteriolar impairment is equally present after exposure to identical doses of TiO₂ (Figure 2). Similarly, leukocyte adhesion and rolling remain elevated at lower doses of ROFA and TiO₂ (Figure 4). These findings reinforce our postulate that the remote biologic effects at the systemic microvascular level after PM exposure are due to the presence of particles in the lung, rather than their inherent pulmonary toxicity, because BAL markers of lung damage were not elevated at doses of < 0.25 mg PM/rat (Table 2, albumin and LDH).

Consistent with our previous study (Nurkiewicz et al. 2004), we report here that systemic microvascular responses after PM exposure are independent of the degree of pulmonary inflammation (as determined by BAL). This is evident from the data in Table 2: BAL from rats exposed to either ROFA or TiO₂ or treated with saline is neither predictably different nor wholly convincing in areas where significance is noted (Table 2, PMNL). However, because activated inflammatory cells may adhere to adjacent tissues or form aggregates too large to recover by BAL or simply involve a very small fraction of the lung, isolated pulmonary “hot spots” may not be represented by our BAL data. Therefore, lung tissue was examined for histopathologic changes by a pathologist to better identify pulmonary pathology after PM exposure. The data in Figure 1 indicate that such “hot spots,” or foci of histiocytic alveolitis, are associated with deposition sites of PM. The collective impression was that this inflammation was focal rather than diffuse (Figure 1C). The increased macrophage activation associated with these foci may be indicated by the dose-responsive increase in AM CL, a measure of macrophage activation.

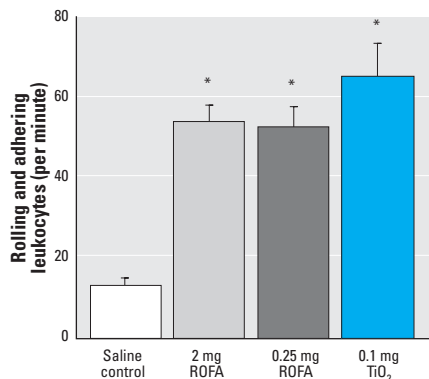


Figure 4. PM exposure increases venular leukocyte rolling and adhesion in the spinotrapezius muscle 24 hr after IT treatment. Venular leukocytes were quantified as rolling and adhering leukocytes per minute in a 200- μ m segment. *n*, number of venules. Saline control, *n* = 26; 2 mg ROFA, *n* = 15; 0.25 mg ROFA, *n* = 18; 0.1 mg TiO₂, *n* = 10. Values are mean \pm SE.

**p* < 0.05 compared with saline control.

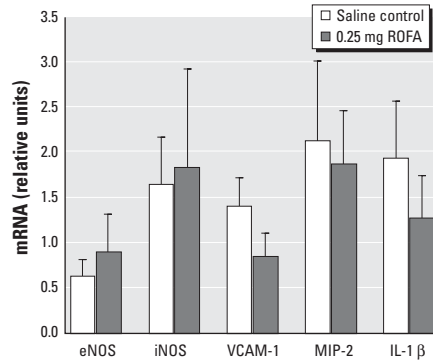


Figure 6. Microvascular inflammatory markers 24 hr after exposure to ROFA: mRNA measurements in microvessels from six saline-treated rats and six rats exposed to 0.25 mg ROFA. After microdissection, vessels from both spinotrapezius muscles of an individual rat were pooled for data collection. Abbreviations: MIP-2, macrophage inflammatory protein; VCAM-1, vascular cell adhesion molecule. Note that neither eNOS nor iNOS message was altered after ROFA exposure.

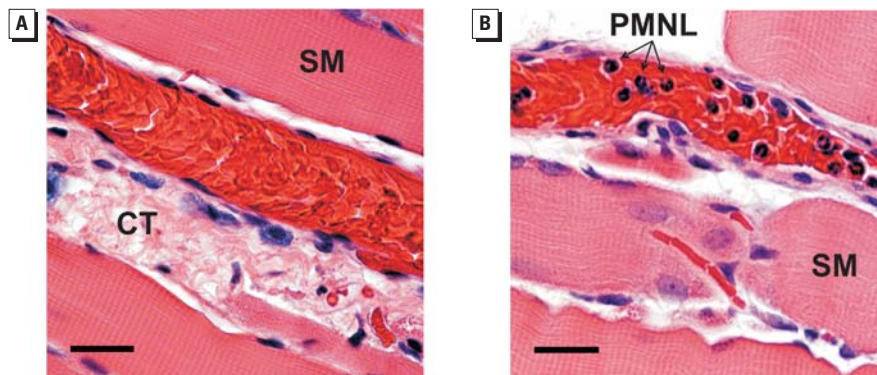


Figure 5. PMNL identification in the spinotrapezius muscle microcirculation of PM-exposed rats 24 hr after IT exposure. (A) Representative H&E-stained section from a saline-treated rat. Abbreviations: CT, connective tissue; SM, skeletal muscle fiber. (B) Representative H&E-stained section from a rat exposed to 0.1 mg ROFA. Note the deeply lobed nuclei that are characteristic of PMNLs. Bars = 25 μ m; similar results were obtained with TiO₂.

Several reports suggest that the autonomic influence on a given tissue is altered after PM exposure (Brook et al. 2004; Chen and Hwang 2005; Wichers et al. 2004). In the present study, we did not observe any differences in blood pressure (Table 1) or arteriolar tone (Table 3). Although this observation does not support the postulate that autonomic activity is altered after PM exposure, it is limited because our experimental data were collected in anesthetized rats. Given this limitation, neurogenic input may still be enhanced by increased receptor sensitivity. The first major finding we report here is that systemic arteriolar α_1 -adrenergic receptor sensitivity is unaltered after PM exposure. This is evident in Figure 3, which shows identical arteriolar constriction produced by iontophoretic application of PHE in both saline-treated and ROFA-exposed rats.

Translocation of PM from the lung to remote sites may also be responsible for adverse cardiovascular effects (Calderon-Garciduenas et al. 2001; Nemmar et al. 2004; Oberdorster et al. 2004). In the present study, ROFA and TiO₂ particles of at least 1 μ m were used, and systemic microvascular changes were measured 24 hr postexposure. There is currently no evidence suggesting that fine PM migrates to systemic sites within this time frame. However, microvascular TiO₂ deposition will be addressed in future studies. A second translocation possibility is that soluble metals from ROFA reach the systemic microcirculation. Soluble metals have been shown to drive many of the pulmonary effects of ROFA (Dreher et al. 1997; Kodavanti et al. 1998; Rice et al. 2001). However, because TiO₂ exhibits the same dose dependence as ROFA (Figures 2 and 4), soluble metals do not appear to be driving the reported microvascular effects.

Our original observations of increased venular leukocyte adhesion and rolling were made in rats exposed to 2 mg ROFA

(Nurkiewicz et al. 2004). This effect is repeatable after exposure to either 0.25 mg ROFA or 0.1 mg TiO₂ (Figure 4). Because this robust response is independent of the PM type or dose, other types of PM may elicit a less pronounced response at lower doses than those used here.

Intravital microscopy is a powerful tool that allows direct observation of leukocyte-venule interaction *in vivo*, but the maximum optical resolution of our system is approximately 1 μ m. Although leukocytes can be easily identified by their characteristic rolling and adhesion in a laminar stream of red cells, further characterization is not possible at this resolution. This issue was resolved via histology of the spinotrapezius muscle (Figure 5), which allowed us to identify the adhering and rolling leukocytes as PMNLs.

Our PCR results indicate that the messages for adhesion factors at the microvascular level are not altered after PM exposure (Figure 6). This suggests that such factors are not altered after exposure to PM, but it is possible that the message quickly increases and then subsides within the 24 hr postexposure period we used. It is also possible that other adhesion factors are involved and/or that the adhesion factors on the leukocytes are altered with no change in the endothelial expression of such factors. Our PCR results also indicated that microvascular eNOS and iNOS messages are not altered after PM exposure. A decrease in eNOS message could have been the cause of the impaired endothelium-dependent dilation, and an increase in iNOS message could have been responsible for the observed microvascular inflammation. However, data shown in Figure 6 do not support the hypothesis that eNOS or iNOS is altered after PM exposure.

The second major finding in this study is that microvascular MPO deposition is associated with PM exposure (Figure 7). Lipopolysaccharide injection in rats produces a diffuse

localization of MPO throughout the aortic endothelium (Eiserich et al. 2002). The MPO was presumed to be secreted by activated leukocytes and taken up by endothelial cells and vascular tissue, independent of neutrophil extravasation. We identified MPO in neutrophils and in the microvasculature of the rat spinotrapezius muscle after treatment of rats with ROFA or TiO₂. Although the MPO was not found in all vessels, it was localized primarily in microvessels within the vicinity of adherent or migrating neutrophils. Given the anatomical and physiologic differences between the aorta and the microcirculation, as well as the heterogeneous nature of a microvascular network, differences in MPO localization are not unexpected. In the spinotrapezius microvasculature, deposition of MPO may also occur during transmigration of the neutrophils. Further immunohistochemical experiments are being done to distinguish endothelial cells from neutrophils because it is possible that the staining we see is not in the endothelial cells but in transmigrating neutrophils. It is also important to note that MPO was identified at a single time point, and future studies must characterize the temporal relationship between PM exposure and MPO deposition. Moreover, future studies will determine the contribution of local MPO deposition to microvascular dysfunction associated with PM exposure.

MPO is the most abundant hemoprotein in leukocytes and comprises approximately 5% of their dry weight (Klebanoff 2005). Therefore, identification of MPO in PMNLs of saline-treated or ROFA-exposed rats is not novel. However, given the significant increase in rolling and adherent PMNLs after ROFA exposure (Figures 4 and 5), it is likely that the systemic microvascular inflammation may be triggered by MPO. This is further supported

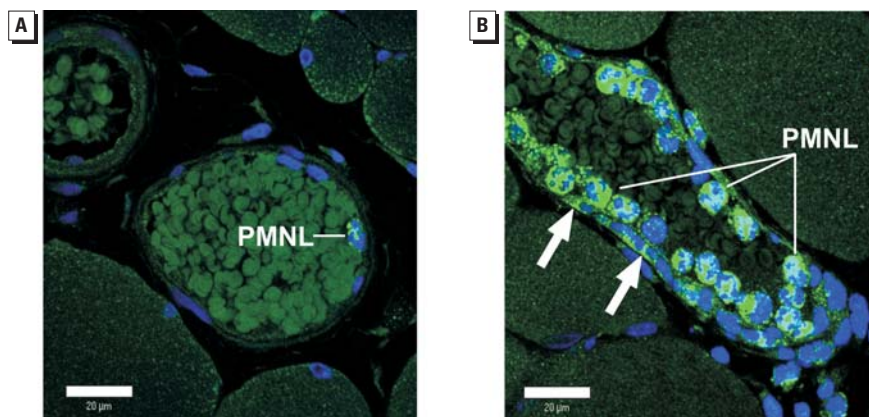


Figure 7. Localization of MPO in the spinotrapezius muscle microcirculation 24 hr after ROFA exposure. Fluorescent antibodies targeted a polyclonal antibody against MPO; nuclei are counterstained blue with DAPI. (A) Representative confocal fluorescent image of a venule from a saline-treated rat. (B) Representative confocal image of a venule from a rat exposed to 0.25 mg ROFA. Note the fluorescence in the microvascular wall indicating the presence of MPO (arrows). Bars = 20 μ m; similar results were obtained with TiO₂.

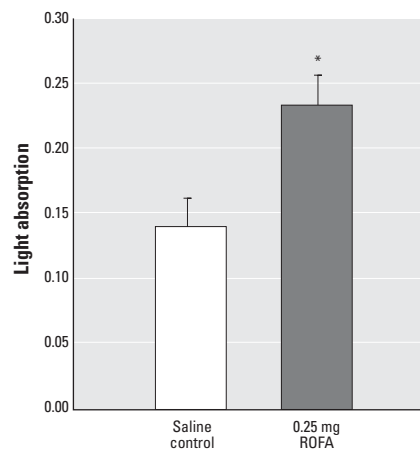


Figure 8. ROFA exposure increases oxidative stress in the systemic microcirculation 24 hr after IT treatment. n = number of vessels. Calculated wall light absorption [$A = \ln(I_p/I_o)$] in microvessels from saline-treated rats ($n = 16$) and rats exposed to 0.25 mg ROFA ($n = 15$) after exposure to 2% TNBT. Values are mean \pm SE. * $p < 0.05$ compared with saline control.

by the observation that firm adhesion of leukocytes to the venular wall is not necessary to alter endothelial intracellular Ca^{2+} concentration or microvascular permeability (Zhu et al. 2005). Moreover, MPO was identified in the microvascular wall of ROFA-exposed rats, whereas it was absent in that of saline-treated rats (Figure 7). Upon deposition in the vascular wall, MPO is preferentially situated in the subendothelial matrix (Baldus et al. 2001), a position in which MPO can ideally interrupt NO signaling between the endothelium and the vascular smooth muscle. MPO may disrupt the influence of NO on microvascular tone from at least two perspectives. MPO generates reactive substrate radicals that consume NO (Eiserich et al. 2002). Alternatively, MPO produces hypochlorous acid that can chlorinate L-arginine and render it unusable by NOS as a substrate for NO production (Zhang et al. 2001).

The third major finding in this study is that oxidative stress is increased in the microvascular wall after PM exposure (Figure 8). The TNBT assay is useful for characterizing general oxidative stress, but it cannot identify specific reactive oxygen species. However, given that leukocyte adhesion and rolling are markedly increased after ROFA exposure (Figure 5) and that MPO is present in the cells and microvascular wall (Figure 7), it is likely that hydrogen peroxide and superoxide are involved in this process. Regardless of which oxygen radicals are elevated after PM exposure, such radicals in the vascular wall have been shown to alter vascular tone and impair endothelium-dependent arteriolar dilation (Lenda et al. 2000; Sato et al. 2003).

Alterations in the vascular reactivity and resting diameter of a large conduit artery after PM exposure have been reported (Brook et al. 2002; O'Neill et al. 2005). Studies by O'Neill et al. (2005) investigated human brachial artery reactivity in diabetic humans after PM exposure and suggested that both endothelium-dependent and -independent arterial dilation are impaired after PM exposure. Conversely, studies by Brook et al. (2002) have reported no change in these vascular reactivity indexes, but they did suggest that the brachial artery constricts by 0.09 ± 0.15 mm after PM exposure. This subtle change had no effect on peripheral resistance because neither systolic nor diastolic blood pressure was altered. O'Neill et al. (2005) reported that endothelium-dependent dilation produced an approximately 6% increase in brachial artery diameter under normal conditions, and this response is decreased by approximately 9% after PM exposure. If we assume a resting brachial artery diameter of 4 mm (Brook et al. 2002), endothelium-dependent dilation under the conditions reported by O'Neill et al. (2005) would cause the brachial artery to dilate to approximately

4.24 mm, and PM exposure would attenuate this dilation to approximately 4.22 mm. The relative contribution of these nominal PM-dependent effects on peripheral resistance would be negligible in a vascular segment that provides little to no vascular resistance. Furthermore, neither study reported brachial artery blood flow data after PM exposure, which would provide some insight into downstream changes in the resistance vasculature. Although the findings by O'Neill et al. (2005) and Brook et al. (2002) do provide valuable biologic end points, the absence of a link to the resistance vasculature makes the physiologic relevance of these findings difficult to assess.

If changes in the reactivity of conduit arteries are not responsible for PM-associated cardiovascular morbidity and mortality, then what vascular events could precipitate such an outcome? Cardiac disturbances and decreases in arterial pressure may occur after pulmonary PM exposure (Wichers et al. 2004). These changes do not appear to be outwardly consistent with our model, in which PM exposure compromises the capacity of the systemic arterioles to dilate. One explanation for this paradox may be that an acute baroreceptor reflex is occurring in response to an increased cardiac afterload. During periods of activity (e.g., walking or stair climbing), cardiac output increases and peripheral dilation is essential to match the metabolic needs of active tissues. An inability to sufficiently reduce peripheral resistance in these circumstances would augment cardiac afterload, thus further increasing arterial pressure. This increased arterial pressure could stimulate an acute baroreceptor reflex that would decrease cardiac output and therefore arterial pressure.

Increases in arterial pressure after PM exposure have also been documented (Chang et al. 2004; Vincent et al. 2001). Our data do not indicate that PM exposure increases arterial pressure, but this possibility cannot be discounted because our data were collected from anesthetized rats. Regardless, the relationship between our findings and those that indicate arterial pressure is increased after PM exposure is more evident. In this case, if our findings in the spinotrapezius muscle are representative of PM exposure effects in other microvascular beds, the inability to decrease peripheral resistance would directly contribute to an increased arterial pressure. In some susceptible populations, such as those with hypertension or vascular disease, this increase in arterial pressure could be fatal if appropriate compensatory mechanisms are also compromised.

Conclusions

The present findings verify our previous report (Nurkiewicz et al. 2004) that systemic endothelium-dependent arteriolar dilation is impaired after pulmonary PM exposure in a dose-dependent manner. Local MPO deposition and

oxidative stress may be mechanisms by which this effect occurs. These findings are consistent with the larger body of evidence that suggests systemic inflammation follows pulmonary PM exposure. Future mechanistic studies will identify the relative contribution of these two effects to the established microvascular dysfunction. It will also be important to determine if these inflammatory effects are localized to target tissues or part of a larger systemic response. The data presented here also suggest that arteriolar adrenergic sensitivity is not affected by PM exposure. Although the systemic microcirculation is capable of overriding neurogenic input, such input still plays a major role in the collective generation of vascular resistance and blood flow distribution. Further studies are necessary to better clarify the influence of peripheral nerves on microvascular function after PM exposure and to determine if this is consistent with a baroreceptor reflex. Because autonomic reflexes can occur rapidly, it will be essential to characterize the temporal relationship of such reflexes after PM exposure.

REFERENCES

- Antonini JM, Roberts JR, Jernigan MR, Yang HM, Ma JY, Clarke RW. 2002. Residual oil fly ash increases the susceptibility to infection and severely damages the lungs after pulmonary challenge with a bacterial pathogen. *Toxicol Sci* 70:110–119.
- Bagate K, Meiring JJ, Cassee FR, Borm PJ. 2004. The effect of particulate matter on resistance and conductance vessels in the rat. *Inhal Toxicol* 16:431–436.
- Baldus S, Eiserich JP, Mani A, Castro L, Figueroa M, Chumley P, et al. 2001. Endothelial transcytosis of myeloperoxidase confers specificity to vascular ECM proteins as targets of tyrosine nitration. *J Clin Invest* 108:1759–1770.
- Brain JD, Knudson DE, Sorokin SP, Davis MA. 1976. Pulmonary distribution of particles given by intratracheal instillation or by aerosol inhalation. *Environ Res* 11:13–33.
- Brook RD, Brook JR, Urch B, Vincent R, Rajagopalan S, Silverman F. 2002. Inhalation of fine particulate air pollution and ozone causes acute arterial vasoconstriction in healthy adults. *Circulation* 105:1534–1536.
- Brook RD, Franklin B, Cascio W, Hong Y, Howard G, Lipsett M, et al. 2004. Air pollution and cardiovascular disease: a statement for healthcare professionals from the Expert Panel on Population and Prevention Science of the American Heart Association. *Circulation* 109:2655–2671.
- Calderon-Garciduenas L, Gambling TM, Acuna H, Garcia R, Osnaya N, Monroy S, et al. 2001. Canines as sentinel species for assessing chronic exposures to air pollutants: part 2. Cardiac pathology. *Toxicol Sci* 61:356–367.
- Campbell A, Oldham M, Becaria A, Bondy SC, Meacher D, Sioutas C, et al. 2005. Particulate matter in polluted air may increase biomarkers of inflammation in mouse brain. *Neurotoxicology* 26:133–140.
- Chang CC, Hwang JS, Chan CC, Wang PY, Hu TH, Cheng TJ. 2004. Effects of concentrated ambient particles on heart rate, blood pressure, and cardiac contractility in spontaneously hypertensive rats. *Inhal Toxicol* 16:421–429.
- Chen LC, Hwang JS. 2005. Effects of subchronic exposures to concentrated ambient particles (CAPs) in mice. IV. Characterization of acute and chronic effects of ambient air fine particulate matter exposures on heart-rate variability. *Inhal Toxicol* 17:209–216.
- Dreher KL, Jaskot RH, Lehmann JR, Richards JH, McGee JK, Ghio AJ, et al. 1997. Soluble transition metals mediate residual oil fly ash induced acute lung injury. *J Toxicol Environ Health* 50:285–305.
- Dye JA, Adler KB, Richards JH, Dreher KL. 1997. Epithelial injury induced by exposure to residual oil fly-ash particles: role of reactive oxygen species? *Am J Respir Cell Mol Biol* 17:625–633.

- Eiserich JP, Baldus S, Brennan ML, Ma W, Zhang C, Tousson A, et al. 2002. Myeloperoxidase, a leukocyte-derived vascular NO oxidase. *Science* 296:2391–2394.
- Fields LE, Burt VL, Cutler JA, Hughes J, Roccella EJ, Sorlie P. 2004. The burden of adult hypertension in the United States 1999 to 2000. A rising tide. *Hypertension* 44:398–404.
- Goldberg MS, Burnett RT, Bailar JC III, Tambllyn R, Ernst P, Flegel K, et al. 2001. Identification of persons with cardiorespiratory conditions who are at risk of dying from the acute effects of ambient air particles. *Environ Health Perspect* 109(suppl 4):487–494.
- Hedley AA, Ogden CL, Johnson CL, Carroll MD, Curtin LR, Flegal KM. 2004. Prevalence of overweight and obesity among US children, adolescents, and adults, 1999–2002. *JAMA* 291:2847–2850.
- Klebanoff SJ. 2005. Myeloperoxidase: friend and foe. *J Leukoc Biol* 77:598–625.
- Kodavanti UP, Hauser R, Christiani DC, Meng ZH, McGee J, Ledbetter A, et al. 1998. Pulmonary responses to oil fly ash particles in the rat differ by virtue of their specific soluble metals. *Toxicol Sci* 43:204–212.
- Kreyling WG, Semmler M, Erbe F, Mayer P, Takenaka S, Schulz H, et al. 2002. Translocation of ultrafine insoluble iridium particles from lung epithelium to extrapulmonary organs is size dependent but very low. *J Toxicol Environ Health A* 65:1513–1530.
- Lenda DM, Boegehold MA. 2002. Effect of a high salt diet on microvascular antioxidant enzymes. *J Vasc Res* 39:41–50.
- Lenda DM, Sauls BA, Boegehold MA. 2000. Reactive oxygen species may contribute to reduced endothelium-dependent dilation in rats fed high salt. *Am J Physiol Heart Circ Physiol* 279:H7–H14.
- Li N, Sioutas C, Cho A, Schmitz D, Misra C, Sempf J, et al. 2003. Ultrafine particulate pollutants induce oxidative stress and mitochondrial damage. *Environ Health Perspect* 111:455–460.
- Nemmar A, Hoet PH, Vanquickenborne B, Dinsdale D, Thomeer M, Hoylaerts MF, et al. 2002. Passage of inhaled particles into the blood circulation in humans. *Circulation* 105:411–414.
- Nemmar A, Hoylaerts MF, Hoet PH, Nemery B. 2004. Possible mechanisms of the cardiovascular effects of inhaled particles: systemic translocation and prothrombotic effects. *Toxicol Lett* 149:243–253.
- Nemmar A, Vanbilloen H, Hoylaerts MF, Hoet PH, Verbruggen A, Nemery B. 2001. Passage of intratracheally instilled ultrafine particles from the lung into the systemic circulation in hamster. *Am J Respir Crit Care Med* 164:1665–1668.
- Nurkiewicz TR, Porter DW, Barger M, Castranova V, Boegehold MA. 2004. Particulate matter exposure impairs systemic microvascular endothelium-dependent dilation. *Environ Health Perspect* 112:1299–1306.
- Oberdorster G, Sharp Z, Atudorei V, Elder A, Gelein R, Kreyling W, et al. 2004. Translocation of inhaled ultrafine particles to the brain. *Inhal Toxicol* 16:437–445.
- Oberdorster G, Sharp Z, Atudorei V, Elder A, Gelein R, Lunts A, et al. 2002. Extrapulmonary translocation of ultrafine carbon particles following whole-body inhalation exposure of rats. *J Toxicol Environ Health A* 65:1531–1543.
- O'Neill MS, Veves A, Zanobetti A, Sarnat JA, Gold DR, Economides PA, et al. 2005. Diabetes enhances vulnerability to particulate air pollution-associated impairment in vascular reactivity and endothelial function. *Circulation* 111:2913–2920.
- Osornio-Vargas AR, Bonner JC, Alfaro-Moreno E, Martinez L, Garcia-Cuellar C, Rosales SP, et al. 2003. Proinflammatory and cytotoxic effects of Mexico City air pollution particulate matter *in vitro* are dependent on particle size and composition. *Environ Health Perspect* 111:1289–1293.
- Pope CA III, Burnett RT, Thun MJ, Calle EE, Krewski D, Ito K, et al. 2002. Lung cancer, cardiopulmonary mortality, and long-term exposure to fine particulate air pollution. *JAMA* 287:1132–1141.
- Porter DW, Ramsey D, Hubbs AF, Battelli L, Ma J, Barger M, et al. 2001. Time course of pulmonary response of rats to inhalation of crystalline silica: histological results and biochemical indices of damage, lipidosis, and fibrosis. *J Environ Pathol Toxicol Oncol* 20(suppl)1:1–14.
- Rao KMK, Meighan T, Porter D, Castranova V. 2004. The sources of inflammatory mediators in the lung after silica exposure. *Environ Health Perspect* 112:1679–1685.
- Rice TM, Clarke RW, Godleski JJ, Al Mutairi E, Jiang NF, Hauser R, et al. 2001. Differential ability of transition metals to induce pulmonary inflammation. *Toxicol Appl Pharmacol* 177:46–53.
- Roberts JR, Taylor MD, Castranova V, Clarke RW, Antonini JM. 2004. Soluble metals associated with residual oil fly ash increase morbidity and lung injury after bacterial infection in rats. *J Toxicol Environ Health A* 67:251–263.
- Salvi S, Blomberg A, Rudell B, Kelly F, Sandstrom T, Holgate ST, et al. 1999. Acute inflammatory responses in the airways and peripheral blood after short-term exposure to diesel exhaust in healthy human volunteers. *Am J Respir Crit Care Med* 159:702–709.
- Samet JM, Dominici F, Currier FC, Coursac I, Zeger SL. 2000. Fine particulate air pollution and mortality in 20 U.S. cities, 1987–1994. *N Engl J Med* 343:1742–1749.
- Sato A, Sakuma I, Gutterman DD. 2003. Mechanism of dilation to reactive oxygen species in human coronary arterioles. *Am J Physiol Heart Circ Physiol* 285:H2345–H2354.
- Schaumann F, Borm PJ, Herbrich A, Knoch J, Pitz M, Schins RP, et al. 2004. Metal-rich ambient particles (particulate matter 2.5) cause airway inflammation in healthy subjects. *Am J Respir Crit Care Med* 170:898–903.
- Schwartz J, Dockery DW, Neas LM. 1996. Is daily mortality associated specifically with fine particles? *J Air Waste Manag Assoc* 46:927–939.
- Schwartz J, Laden F, Zanobetti A. 2002. The concentration–response relation between PM_{2.5} and daily deaths. *Environ Health Perspect* 110:1025–1029.
- Tan WC, Qiu D, Liam BL, Ng TP, Lee SH, van Eeden SF, et al. 2000. The human bone marrow response to acute air pollution caused by forest fires. *Am J Respir Crit Care Med* 161:1213–1217.
- U.S. Census Bureau. 2004. U.S. Interim Projections by Age, Sex, Race, and Hispanic Origin. Available: <http://www.census.gov/ipc/www/usinterimproj/> [accessed 19 September 2005].
- van Eeden SF, Tan WC, Suwa T, Mukae H, Terashima T, Fujii T, et al. 2001. Cytokines involved in the systemic inflammatory response induced by exposure to particulate matter air pollutants (PM₁₀). *Am J Respir Crit Care Med* 164:826–830.
- Veronesi B, Oortgiesen M, Roy J, Carter JD, Simon SA, Gavett SH. 2000. Vanilloid (capsaicin) receptors influence inflammatory sensitivity in response to particulate matter. *Toxicol Appl Pharmacol* 169:66–76.
- Vincent R, Kumarathasan P, Goegan P, Bjarnason SG, Guenette J, Berube D, et al. 2001. Inhalation toxicology of urban ambient particulate matter: acute cardiovascular effects in rats. *Res Rep Health Eff Inst* 104:5–54.
- Wichers LB, Nolan JP, Winsett DW, Ledbetter AD, Kodavanti UP, Schladweiler MC, et al. 2004. Effects of instilled combustion-derived particles in spontaneously hypertensive rats. Part I: Cardiovascular responses. *Inhal Toxicol* 16:391–405.
- Zhang C, Reiter C, Eiserich JP, Boersma B, Parks DA, Beckman JS, et al. 2001. L-Arginine chlorination products inhibit endothelial nitric oxide production. *J Biol Chem* 276:27159–27165.
- Zhu L, Castranova V, He P. 2005. fMLP-stimulated neutrophils increase endothelial [Ca²⁺]_i and microvessel permeability in the absence of adhesion: role of reactive oxygen species. *Am J Physiol Heart Circ Physiol* 288:H1331–H1338.